Pharmacogn. Mag.
A multifaceted peer reviewed journal in the field of Pharmacognosy and Natural Products
www.phcog.com | www.phcog.net

ORIGINAL ARTICLE

Zerumbone Ameliorates the Induced Atherosclerosis-Initiated Inflammatory Conditions through Suppression of Proinflammatory Mediators and Inflammatory Cytokines

Hemn Hassan Othman[1,2]*, Heshu Sulaiman Rahman[3,4], Sherwan Hamasalih Omer[3], Syam Mohan[5], Mohammed Abdulabbas Hasan[6], Kawa Amin[7], Nagi A. AL.Haj[8], Hareth Yahya Ahmed[9], Noordin Mohamed Mustapha[1]

[1]Department of Microbiology and Pathology, Faculty of Veterinary Medicine, Universiti Putra Malaysia, 43400 UPM Serdang, Selangor, Malaysia, [2]Department of Pharmacology and Toxicology, College of Pharmacy, [3]Department of Physiology, College of Medicine, University of Sulaimani, 46001 Sulaimaniyah, [4]Department of Medical Laboratory Sciences, College of Health Sciences, Komar University of Science and Technology, Sarchinar District, Sulaimaniyah, Republic of Iraq, [5]Substance Abuse and Toxicology Research Center, Jazan University, Jazan, Saudi Arabia, [6]Biology Science Department, College of Education for Women, Thi-Qar University, Thi-Qar, [7]Department of Microbiology, College of Medicine, University of Sulaimani, 46001 Sulaymaniyah, Republic of Iraq, [8]Faculty of Medicine and Health Sciences, Sana'a University, Sana'a, Yemen, [9]Institute of Bioscience, Universiti Putra Malaysia, 43400 UPM Serdang, Selangor, Malaysia

Submitted: 18-Dec-2020 Revised: 22-Apr-2021 Accepted: 05-Aug-2021 Published: 11-Nov-2021

ABSTRACT

Background: Zerumbone (ZER) is a naturally occurring monosesquiterpine and dietary compound from *Zingiber zerumbet* Smith, an edible ginger. It has been shown to possess anti-inflammatory activities. Inflammation plays an important role in all stages of atherosclerosis. However, little is known about ZER's anti-inflammatory role in atherosclerosis. **Objectives:** This study investigated the anti-inflammatory effect of ZER in mitigating the formation and development of early atherosclerotic lesions in rabbits fed with high-cholesterol diet. **Materials and Methods:** A total of 72 New Zealand White rabbits were used in two experimental studies carried out at different times. The first experiment was carried out to investigate the prophylactic effects of ZER in preventing premature atheromas plaque formation. In contrast, the second experiment was carried out to assess the therapeutic efficacy of ZER in reducing atheromas lesion progression and dissemination. **Results:** ZER significantly ($P < 0.05$) reduced the inflammatory response through suppression of proinflammatory mediators (nuclear factor kappa-light-chain-enhancer of activated B-cells, inducible nitric oxide synthase, and cyclooxygenase-2), which leads to decrease in the secretion of inflammatory cytokines (tumor necrosis factor alpha, interleukin [IL]-6, IL-1, and IFN-γ) evaluated by western blotting and enzyme immunoassay techniques, respectively. Conversely, suppression and reduction of inflammatory mediators then contribute to minimizing macrophages recruitment, which is evident by immunohistochemistry and immunofluorescent assays of regulation of ACE2 and morphogenesis 11 (RAM-11). In addition, ZER significantly ($P < 0.05$) reduces the expression of RAM-11 in the intimal plaque in all supplemented and treated groups in a dose-dependent manner, which is much profound in the prophylactic trial. **Conclusion:** The results of the study clearly concluded that ZER is an anti-inflammatory agent alone as a prophylactic measure or in combination with simvastatin as a remedy. In effect, dietary consumption of ZER can be viewed as beneficial in preventing and attenuating early atherosclerosis.

Key words: Atherosclerosis, inflammation, nuclear factor kappa-light-chain-enhancer of activated B-cells, rabbit model, regulation of ACE2 and morphogenesis 11, zerumbone

SUMMARY

- *Zingiber zerumbet* L. Smith or Lempoyang is an edible ginger that has been traditionally used in foods and beverages as an oriental spice, food-flavoring agent, and appetizer. It contains zerumbone (ZER) as the active compound that possesses multiple biomedical properties, such as antiproliferative, antioxidant, anti-inflammatory, and anticancer activities. In the present study, high-cholesterol diet induced atherosis through elevation in percentage and density of regulation of ACE2 and morphogenesis 11 (RAM-11). Thus, the inflammatory pathway was investigated in White New Zealand Rabbits. ZER is proved to be effective in reducing atherosis through a decrease in RAM-11 expression in the intimal plaque in all supplemented and treated animals.

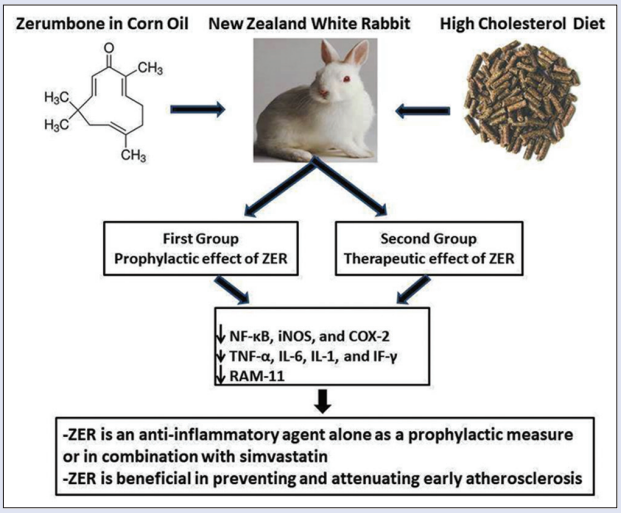

Abbreviations used: BW: Body weight; COX-2: Cyclooxygenase-2; CRP: C-reactive protein; DTAF: Diaminotriazinylaminofluorescein; HCD: High cholesterol diet; HRP: Horseradish peroxidase; ICAM: Intercellular adhesion molecules; IF: Immunofluorescent; IF-γ: Interferon gamma; IHC: Immunohistochemistry; IL: Interleukin; iNOS: Inducible nitric oxide synthase; NF-κB: Nuclear factor kappa-light-chain-enhancer of activated B-cells; NZW: New Zealand White; PBST: Phosphate-buffered saline Tween; RAM-11: Regulation of ACE2 and morphogenesis 11; RIPA: Radioimmunoprecipitation assay; SIM: Simvastatin; TNF-α: Tumor necrosis factor alpha; VCAM: Vascular cell adhesion molecule; ZER: Zerumbone.

Correspondence:

Dr. Hemn Hassan Othman,
Department of Pharmacology and Toxicology,
College of Pharmacy, University of Sulaimani,
46001 Sulaimaniyah, Republic of Iraq.
E.mail: hemn.othman@univsul.edu.iq

DOI: 10.4103/pm.pm_549_20

Access this article online
Website: www.phcog.com
Quick Response Code:

Cite this article as: Othman HH, Rahman HS, Omer SH, Mohan S, Hasan MA, Amin K, *et al*. Zerumbone ameliorates the induced atherosclerosis-initiated inflammatory conditions through suppression of proinflammatory mediators and inflammatory cytokines. Phcog Mag 2021;17:419-27.

INTRODUCTION

Atherosclerosis is a complex, chronic, proliferative, and accumulative inflammatory mayhem with intricate cellular and molecular immune mechanisms.[1] In general, transcriptional factors, proinflammatory cytokines, growth factors, adhesion molecules, and chemotactic proteins that are released by chronic inflammatory cells play crucial roles in the pathogenesis of atherosclerosis, which results in monocytes' recruitment and vascular smooth muscle cells' proliferation–migration and transformation to foam cells in the intimal layer.[2,3]

All classes of activated cells, including lipid-laden macrophages (foam cells), adhered monocytes, T-cells, and transmigrated smooth muscle cells, will release proinflammatory mediators such as interleukin-6 (IL-6), tumor necrosis factor-alpha (TNF-α), and C-reactive protein that upregulates overexpression of adhesion molecules such as vascular cell adhesion molecules and intercellular adhesion molecules, which mediate adhesion of more leukocytes to the defect endothelium.[4] Continuous recruitment of circulating leukocytes into the vessel wall and the expression of proinflammatory cytokines play crucial roles in the pathogenesis of atherosclerosis.[5] Recent investigations in basic science have established a fundamental role of inflammation in mediating all stages of atherosclerosis starting from initiation, progression, and eventually, the advanced thrombotic complications. These new findings provide significant links between traditional risk factors and the mechanisms of atherogenesis.[6]

Zerumbone (ZER) [Figure 1] is a naturally occurring monosesquiterpine from *Zingiber zerumbet* Smith.[7,8] ZER is the most abundant constituent (up to 75%) of the essential oil from the rhizomes and possess anti-inflammatory[9] and antiproliferative potential.[10] ZER has been demonstrated to attenuate inducible nitric oxide synthase (iNOS) and cyclooxygenase-2 (COX-2) expression via modulation of nuclear factor kappa-light-chain-enhancer of activated B-cells (NF-κB) activation.[9] Based on the phytotherapeutic effects of ZER against proliferative and inflammatory disorders, it has been approved that ZER can suppress some cytokines that play a significant role in the initiation of atherogenesis, such as IL-6[11] and TNF-α.[12,13]

Earlier, we have established that the oral administration of ZER can regulate the food intake and body weight of animals, which eventually reduced the plaque formation together with a reduction in serum lipid profile, suppression of oxidative damage, and alleviated atherosclerosis lesions.[14] The present study was designed to evaluate the anti-inflammatory efficacy of ZER as a protective and therapeutic measure in preventing and reducing the early-developed atherosclerotic lesion in the aorta of rabbits fed with high-cholesterol diet.

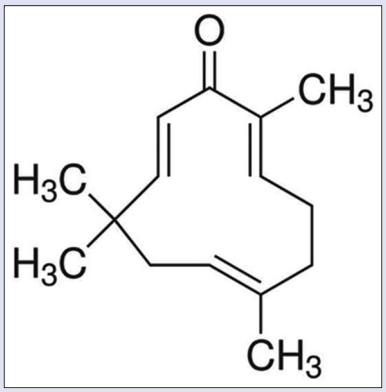

Figure 1: Chemical structure of ZER. ZER: Zerumbone

MATERIALS AND METHODS

Zerumbone extraction and preparation

ZER was extracted using the hydrodistillation method according to the a previous method.[14] Briefly, about 30 kg of fresh rhizomes of *Z. zerumbet* was obtained from a local market in Kuala Lumpur, Malaysia. *Z. zerumbet* was identified at the Department of Biodiversity, Institute of Bioscience, Universiti Putra Malaysia (UPM), and a voucher specimen was deposited in a herbarium. After cleaning and slicing, the rhizomes were placed in a steam hydrodistiller containing purified water and heated. Then, the steamed volatile oil was collected, mixed in equal volume with absolute hexane (Sigma-Aldrich Co, St Louis, MO, USA), and placed in a fume hood to allow hexane evaporation and ZER crystallization. Crystals of ZER (1.3 g/kg of rhizome) were aliquoted and kept at 4°C for further use. The extract was checked for its purity by using HPLC. The obtained single peak confirmed that the compound is more than 99.31% pure. The spectra were published earlier online.[14]

Regarding fresh ZER solution preparation for daily oral dose, pure ZER crystals were dissolved in corn oil using sonicator (Emerson Industrial Group, Danbury, CT, USA) for exactly 15 min at 40°C. The 0.4% (8 mg/kg BW), 0.8% (16 mg/kg BW), and 1% (20 mg/kg BW) ZER solutions were prepared by dissolving 100, 200, and 250 mg ZER crystals in 25 mL corn oil according to the protocol described previously.[14]

Preparation of simvastatin solution

Fresh SIM solution was prepared daily by dissolving a SIM tablet (5 mg for preventive and 15 mg for therapeutic trial) (Zocor®; Merck and Co, Inc., Whitehouse Station, NJ, USA) in 2.0 mL distilled water after vigorous shaking for few minutes at room temperature.

Preparation of 1% high-cholesterol diet

A high-cholesterol diet (HCD) was designed as an atherogenic diet to induce experimental atherosclerosis according to the previous method.[14] Briefly, each rabbit received a daily 1.0 g sheep wool isolated pure cholesterol powder (Sigma-Aldrich) dissolved in 100 mL chloroform (Avantor Performance Materials, Center Valley, PA, USA) with 100 g of pellets after the mixture was placed in an air-ventilated oven at 40°C (Sheldon Manufacturing, Inc., Cornelius, OR, USA) for 24 h to complete the evaporation of chloroform.

Animals

Healthy male New Zealand White (NZW) rabbits aged 10–12 weeks and weighed 1.5–2.0 kg were used for the study Animals were purchased from A-Sapphire Enterprise (Selangor, Malaysia), acclimatized in an air-conditioned room at 22°C–25°C for 7 days, and provided free access to food and water. All animals were individually caged under normal experimental laboratory conditions in a 12-h light/12-h dark cycle and received 100 g rabbit chow diet and water *ad libitum*.

Experimental design and animal treatment

A total of 72 NZW rabbits were divided randomly into two experimental groups (prophylaxis and treatment) carried out at a different time. The interval between the experiments was 8 weeks. The first experiment was designed to investigate the prophylactic efficacy of ZER supplementation in preventing early development and the establishment of atherosclerotic lesions induced by HCD. A total of 30 healthy NZW rabbits were randomly distributed into five groups comprising 6 animals each, including control (CN), hypercholesterolemic diet (HCD), and ZER-preventive (ZPI, ZPII, and ZPIII) groups. Animals in the CN group were fed 100 g normal rabbits chow daily and those in the HCD group received 1% HCD daily for 10 weeks, while those in ZPI, ZPII, and ZPIII

groups received 1% HCD together with ZER at the dose of 8, 16, and 20 mg/kg, respectively, for precisely 10 weeks.

The second experimental study investigated the therapeutic effects of ZER treatment in reducing the progression of newly established atherosclerotic lesions in rabbits fed HCD, wherein 42 rabbits equally assigned into seven groups comprising 6 animals each, including CN, high-cholesterol diet (HCD), ZER treatment groups (ZI, ZII, and ZIII), SIM group (SG), and ZER-SIM combination group (ZSG). All rabbits except those in the CN received 1% HCD for 10 weeks. After 10 weeks of feeding, the therapeutic regimen was initiated for an additional period of 4 weeks. Animals in the ZI, ZII, and ZIII groups received ZER at the dose of 8, 16, and 20 mg/kg, respectively. However, those in the SG and ZSG groups received 15 mg/kg SIM and 5 mg/kg SIM plus 8 mg/kg ZER, respectively. To achieve an optimal effect, ZER was given on an empty stomach (early morning) while SIM in the evening as prescribed by the manufacturer. Both ZER and SIM were given to animals by gavage using a force-feeding needle.

At the end of the study, animals were sacrificed and thoracic aortas were collected for each experiment. The animals were initially placed and immobilized inside a restrainer and later anesthetized with a mixture of ketamine (20 mg/kg BW) and xylazine (10 mg/kg BW). Injected rabbits were left for 5 min to allow complete general anesthesia, after that followed by an overdose 3 mL of sodium pentobarbital (140 mg/kg BW) via intracardial infusion to obtain optimum humane euthanasia. Sections from aortic arches and thoracic aortas were carefully taken out, cleaned from surrounding fat, and washed out from blood gently with physiological saline (0.9%). Approximately 10–20 mm of aortic arches and/or thoracic aortas were fixed in 10% buffered formalin at least 48 h for immunoperoxidase assay (immunohistochemistry [IHC] and immunofluorescence [IF]).

All experimental procedures were approved following the Animal Care and Use Committee guides implemented by the Faculty of Veterinary Medicine, UPM, with a reference number (UPM/FPV/PS/3.2.1.551/AUP).

Immunohistochemistry assay

The IHC analysis was performed using a Dako REAL™ EnVision™ Detection System – horseradish peroxidase (HRP), peroxidase/(DAB+), rabbit/mouse kit (Dako K5007, Denmark) following the manufacturer's instruction. Initially, the paraffin-embedded arteries were cross-sectioned into 4 μm thick pieces at 5 mm intervals, baked in oven at 60°C for 45–60 min, and rehydrated with gradation series of xylene and ethanol, respectively. For macrophage identification as a major inflammatory cell contribute mainly in the process of atherogenesis, a monoclonal antirabbit macrophage antibody (regulation of ACE2 and morphogenesis 11 [RAM-11], code M0633, DAKO, Denmark) was applied. Non-specific antibody binding was blocked by incubation of the tissue section for 10 min with proteinase K at room temperature. Endogenous peroxidase activity was extinguished by incubation of the sections in 3% hydrogen peroxide (H2O2) for 5 min. Then, rinsed with distilled water and washed gently by Tris-buffer solution with 0.05% Tween-20 twice. Primary mouse-monoclonal antirabbit macrophage RAM-11 antibody was diluted at 1:50 according to the manufacturer's protocol and applied to the sections after determination with the blocking pen for 30 min at room temperature. Following the same washing process, sections were incubated for 30 min at room temperature with dextran backbone peroxidase-conjugated coupled with goat secondary antibody against rabbit and mouse immunoglobulins (Ig) (DAKO REAL, EnVision/HRP, Rabbit/Mouse); subsequently, the reaction was visualized via staining the sections with 3,3'-diaminobenzidine tetrahydrochloride in buffered solution of H_2O_2 as preservative for 10 min.

Finally, sections were counterstained with hematoxylin and dehydrated in graduated ethanol alcohol. Specimens were mounted and cover slipped using DPX as a nonaqueous permanent mounting medium. In each experiment, negative controls without the primary antibody or with an unrelated antibody were included to check for non-specific staining.

Immunofluorescence assay

IF staining of formalin-fixed paraffin-embedded tissue was carried out using goat polyclonal secondary antibody to mouse IgG-H and L (FITC) (Abcam® ab6785, Cambridge, UK) following the manufacturer's instruction. Paraffin-embedded arteries were cross-sectioned into 4 μm thick pieces at 5 mm intervals and baked in oven at 60°C for 30 min. After cooled down, the sections were placed under ultraviolet light for about 30–60 min to bleach the autofluorescence pigments. Then, they were deparaffinized and rehydrated with two changes of xylene each 5 min and gradation series of ethanol (100%, 100%, 95%, 70%, and 50%) each 3 min, respectively. Principally, for macrophage identification, a monoclonal antirabbit macrophage antibody (RAM-11, code M0633, DAKO, Denmark) was applied as a primary antiserum. Antigen was demasked and retrieved simultaneously with blocking of non-specific antibody binding by incubation of the tissue section for 10 min with proteinase K at room temperature. Sections were washed gently with phosphate-buffered saline-Tween 20 (0.05%) solutions (PBST solution) twice every 5 min. Primary antibody, mouse-monoclonal antirabbit macrophage RAM-11 was diluted 1:50 and applied to the sections after determination with the blocking pen for 30 min at room temperature.

Later on, sections were washed in PBST solution and incubated for 30 min in a dark chamber with goat polyclonal secondary antibody to mouse IgG-H and L (FITC) diluted 1:100 and conjugated with diaminotriazinylaminofluorescein (fluorochromes/protein ratio: 3.3 moles FITC per mole of goat IgG). Subsequently, sections were rinsed with PBST twice and then were cover-slipped in fluorescence mounting medium to minimize the fading of immunofluorescence dye during microscopy. Finally, coverslip edges were appropriately sealed with clear nail polish, and sections were stored at 2°C–8°C in a special dark slide box until viewing and capturing photographs using a light microscope.

Immunoquantitative evaluation of antimacrophage regulation of ACE2 and morphogenesis 11

Evaluation of RAM-11 IHC staining was done based on the number of immunoreactive cells that possess brown color in each microscopic field using an image analyzer microscope (Olympus B × 51TF Japan). Briefly, each section within a slide divided into four fields. The labeling index was expressed as the number of cells with positive brownish staining per 100 counted cells in each field. The immunosemiquantitative assessment of RAM-11 was calculated by multiplication of the percentage of immunoreactive cells (quantity score) with the staining intensity (staining intensity score). Quantity score was calculated based on the following scoring system: No staining is scored as 0, 1%–10% of cells stained scored as 1, 11%–50% as 2, 51%–80% as 3, and 81%–100% as 4. Staining intensity is rated on a scale of 0–3, with 0 = negative; 1 = weak; 2 = moderate, and 3 = strong.

Quantitative assay of immunofluorescent cells

Quantitative labeling index assessment of apoptotic and immunofluorescent cells for RAM-11 was done based on the number of green fluorescein reactive cells in the single microscopic field using the image analyzer fluorescence microscope (Nikon, ECLIPSE 80i, Japan), following the protocol of IHC-reactive cells quantification.[15]

Immunoblotting

Protein extraction and quantification

Freshly excised aortic tissues were cut into small pieces and snap-freeze in liquid nitrogen for 30 s. Then, 100 mg of tissue was transferred to Eppendorf tube, and about 100 µL radioimmunoprecipitation assay lysis buffer (Thermo Scientific, USA) containing 1.0 µL protease inhibitor cocktail (Sigma Aldrich, USA) was added, homogenized for 30 s, and incubated at 4°C for 1 h with agitation. Later on, the lysate was clarified by spun down at 10,000 rpm for 10 min (Eppendorf, USA); supernatant-contained different amounts of proteins were collected and transferred into a new Eppendorf tube. The concentration of extracted proteins was quantified using the Bradford protein assay kit following the instruction of a manufacturing company without any modification (BioRad, USA), while bovine serum albumin (Sigma Aldrich, USA) was used as standard. Plates were read at 405 nm using ELISA plate reader (Biotech, Inc., USA), and the standard curve was plotted. At last, protein suspensions were aliquoted into PCR tubes (BioRad, USA) and stored at −80°C for further analysis by sodium dodecyl sulfate-polyacrylamide gel electrophoresis (SDS-PAGE).

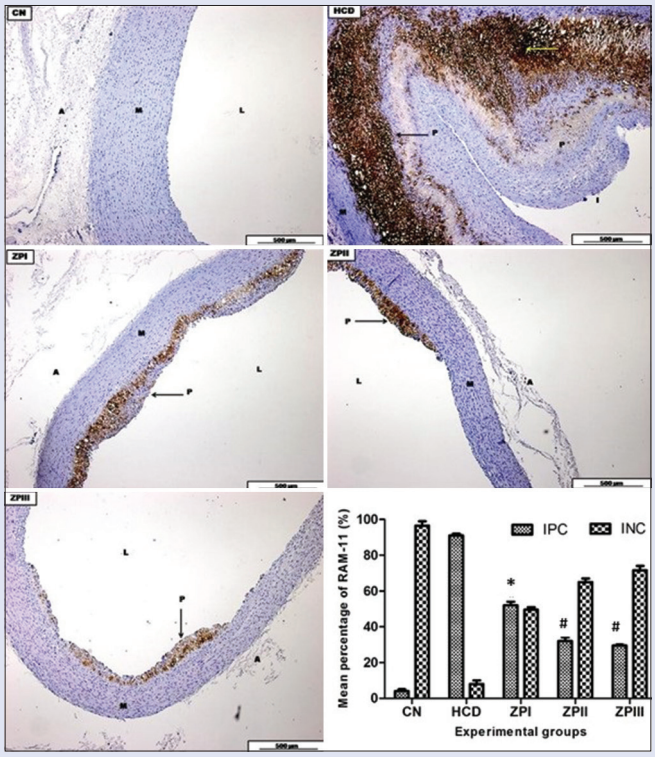

Figure 2: The photomicrograph of thoracic aortas represents immunohistochemical staining with RAM-11 antibody from CN, HCD, ZPI, ZPII, and ZPIII groups. CN shows no IPC. HCD displays massive and diffuse IPCs within thick rising plaque (p) indicated by deep brownish-stained macrophages (black and yellow arrows). Aortas in ZPI, II and III groups demonstrate a significant reduction in plaque size (p) and the intensity of brownish color RAM-11 immunopositive foam cells compare to the thick plaque in HCD (black arrows). There is no reaction in the muscularis layer (m). Bar graph represents the quantification assay of IPC and INC cells. *indicates a statistical significance at $P < 0.05$ and #indicates a statistical significance at $P < 0.01$. L: Lumen; M: Media; A: Adventitia. Scale bars: 500 µm. CN: Control group; RAM-11: Regulation of ACE2 and morphogenesis 11; ZP: ZER-preventive; ZER: Zerumbone; IPC: Immunoreactive-positive cells; INC: Immunoreactive-negative cells

Sample preparation

Aliquoted protein lysates were removed from freezer, allowed to thaw on ice for 20 min, diluted with PBS to the required concentration (25 µg per sample), and vortexed (VELP Scientifica, Italy) for exactly 10 s at room temperature before heated at 99°C using thermo-block (FALC, Italy) with equal amount of 4X electrophoresis sample buffer working solution (BioRad, USA) for 5 min to allow denaturation of protein. After that, they were vortexed again for 10 s and immediately transferred to the ice to be load into gel wells for SDS-PAGE.

Western blotting

An equal amount of protein (25 µg) was resolved and separated based on molecular weight by electrophoresis in an electric field (100 V for 30 min followed by 150 V for 1 h) at 10% SDS-PAGE system (BioRad, USA). The broad (11.0–240.0 kDa) prestained protein molecular weight ladder (GeneDirex, USA) was used for monitoring the protein migration during SDS-PAGE as well as for checking the protein transfer efficiency. Then, proteins were transferred and blotted on to the PVDF membrane (BioRad, USA). Later on, membranes were blocked sequentially for 1 h in blocking solution at room temperature on a belly dancer. Membranes were washed with PBST and probed with specific primary antibodies overnight at 4°C on a belly dancer. Primary antibodies against NF-κB, COX-2, iNOS, Bcl-2, and Bax (Abcam, USA) were used. The next day, membranes were washed 6 times, 10 min each with PBST at room temperature on a belly dancer. Followed this, incubation with goat–antirabbit IgG conjugated to HRP secondary antibody (Abcam, England) at room temperature on belly dancer was done, and membranes were rewashed 6 times, 10 min each with PBST for 1 h at room temperature on a belly dancer.

The immunoreacted protein bands were developed and detected using chemiluminescence blotting substrate kit (ECL Western blot substrate, Abcam, England), and chemiluminescence image analyzer system (Chemi-Smart, Vilber Lourmat, Germany) was used for viewing and observing of the membrane. The results were expressed in standard units. The bands obtained were quantified with Image J software (BioTechniques, USA).

Enzyme-linked immunosorbent assay

Serum proinflammatory cytokine concentrations were determined using a commercially available kit (CUSABIO, BIOTECH, China) following the manufacturer's instruction. Briefly, 100 µL of rabbit's serum and TNF-α, IFN-γ, IL-1, and IL-6 standards in serial concentrations ([5000, 2500, 1250, 625, 312.5, 156.25, 78.13, and 0], [4000, 2000, 1000, 500, 250,125, 62.5, and 0], [1000, 500, 250, 125, 62.5, 31.2, 15.6, and 0], and [1000, 500, 250, 125, 62.5, 31.2,15.6, and 0], respectively) were added in duplicates to each well coated with TNF-α-, IFN-γ-, IL-1-, and IL-6-specific antibodies and then incubated for 2 h at 37°C. Serum was removed, and 100 µL of biotin-labeled with TNF-α-, IFN-γ-, IL-1-, and IL-6-specific antibody conjugates was added and incubated for 1 h at 37°C.

Each well was aspirated and washed three times with wash buffer, HRP-avidin (100 µL) was added then incubated for 1 h at 37°C, and the plates were washed again for 5 more times with the washing buffer. The plates blotted on a clean filter paper for the complete removal of washing fluid, then TMB substrate (90 µL) were added to each well and incubated for 25 min at 37°C. Stop solution (50 µL) was added to each well and then the optical density (OD) was determined by ELISA reader set to 450 nm within 5 min. The duplicate readings were taken the average for each standard, and the sample then subtracted the average zero standard OD, using the professional soft curve exert 1.4 to make a standard curve.

Statistical analysis

All descriptive statistical analysis was performed using Statistical Package for the Social Sciences (SPSS) version 25.0 (SPSS Inc., Chicago, USA). The data were analyzed and presented as mean ± standard error mean of six animals. Means of multiple groups were compared by Tukey's HSD *post hoc* test and $P < 0.05$ was considered statistically significant. Statistical differences between the groups were evaluated using the one-way analysis of variance test.

RESULTS

Protective effect of zerumbone against HCD-induced atherosclerosis

Immunohistochemistry assay

There were a higher percentage and density of RAM-11 in the HCD group than the CN group [Figure 2]. In respect to macrophage biomarker, all ZER-supplemented groups showed significant ($P < 0.05$) reduction in RAM-11-positive cells represented by considerable alleviation in the percentage of immunoreactive-positive brownish cells and plaque size compared to HCD group, in which the results are more significant ($P < 0.01$) in ZPII and ZPIII groups [Figure 2].

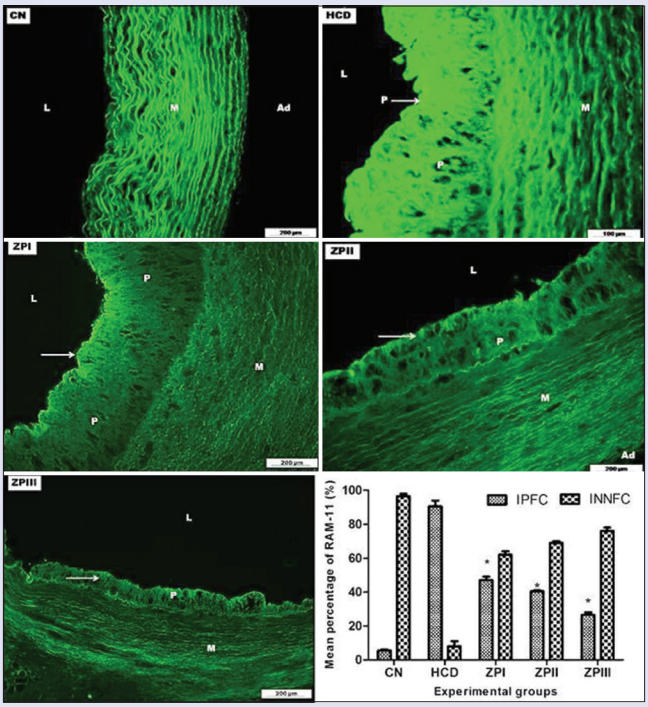

Figure 3: Photomicrograph of thoracic aortas from CN, HCD, ZPI, ZPII, and ZPIII groups symbolize immunoflourescent staining with RAM-11 antibody. Control group shows no immunopositive reaction. HCD group demonstrates pronounced IPFCs with increasing intensity and percentage of greenish-fluorochrome foam cells in the intimal plaque (p). Aortas in ZPI, II and III groups demonstrate a significant reduction in the macrophage-derived foam cells within the tunica intima compare to HCD group, indicated by the low intensity of greenish-fluorochrome immunopositive RAM-11 cells in the intimal plaque (p) (white arrows). Bar graph represents (IPFC) and (INNFC) cells of macrophage-specific protein biomarker RAM-11. *indicates statistical significance compared to HCD at $P < 0.05$. L: Lumen; M: Media; A: Adventitia. Scale bars: 200 µm. CN: Control group; RAM-11: Regulation of ACE2 and morphogenesis 11; ZP: ZER-preventive; ZER: Zerumbone; IPC: Immunoreactive-positive cells; INC: Immunoreactive-negative cells; IPFC: Immunopositive fluorescent cells; INNFC: Immunonegative nonfluorescent cells

Immunofluorescent assay

The results of this test demonstrated the high intensity of the IF-reactive–positive greenish foam cells of the HCD group compared to negatively immunoreactive cells in the CN group [Figure 3]. In general, the data showed expressive suppression in the intensity of greenish-fluorochrome color expression in the intimal plaque of ZER-supplemented groups compared to the HCD group [Figure 3].

Western blot assay (quantification of protein expression)

Generally, β-actin was used as a loading control, which showed relatively equal intensity bands that confirming the equal protein concentration in all tested samples. As a result, protein quantification analysis in the current experiment showed that there was a significant ($P < 0.05$) downregulation in protein expression of NF-κB as well as in the inducible enzymes COX-2 and iNOS in the aortic tissue of ZPI, ZPII, and ZPIII groups in a dose-dependent manner comparable to that of HCD group [Figure 4a and b].

Seroimmunological analysis of proinflammatory cytokines (ELISA)

ZER showed potent and significant anti-inflammatory effects in reducing serum proinflammatory cytokines being analyzed serologically by the

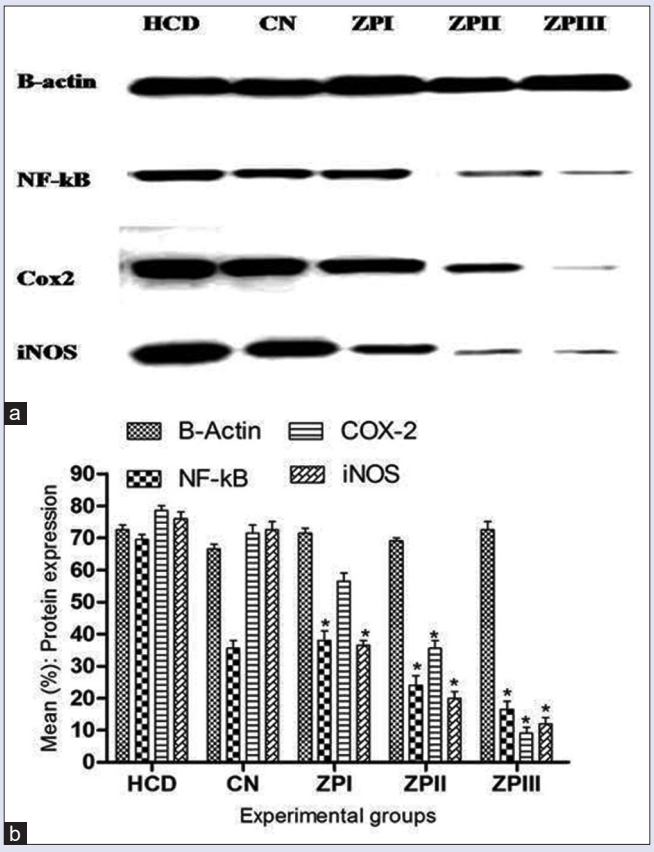

Figure 4: (a) Western blot image analysis from aortic tissue for NF-κB, COX-2, and iNOS. All ZER-supplemented groups show a significant reduction in the protein band thickness, indicating the downregulation of protein expression. (b) Bar graph represents protein transcription analysis in aortic tissue by Western blotting assay using Image J software. Data reveal significant ($P < 0.05$) suppression of NF-κB, COX-2, and iNOS proteins in ZER-preventive groups compare to that of HCD group. ZER: Zerumbone; NF-κB: Nuclear factor kappa-light-chain-enhancer of activated B-cells; COX-2: Cyclooxygenase-2; iNOS: Inducible nitric oxide synthase

ELISA test. The obtained data demonstrated that the mean percentage values of TNF-α, IFN-γ, IL-1, and IL-6 were significantly ($P < 0.05$) reduced in all ZER-supplemented groups in a dose-dependent manner comparable to that in HCD group, wherein the result is more significant ($P < 0.05$) in ZPIII compared to ZPI and ZPII groups [Table 1].

Therapeutic efficacy

Immunohistochemistry assay

The CN group shows no evidence of positive reaction compared to the HCD group [Figure 5]. As a result, ZER-treated groups display a pronounced drop in the density of RAM-11 immunoreactive-positive brownish cells, together with a notable reduction in the plaque size [Figure 5]. Similarly, the SG group shows evidence of foam cell reduction compared to the HCD group; however, the higher antimacrophage effect was observed in the ZSG group [Figure 5].

Immunofluorescent assay

There was no immunopositive fluorescent reaction in the CN group compared to the HCD group. Furthermore, Figure 6 shows a pronounced reduction in the intensity of greenish-fluorochrome foam cells in the intimal plaque of ZI, ZII, and ZIII groups in a dose-dependent manner compared to the HCD group. More significant ($P < 0.05$) effect was noticed in the ZSG group in comparison to the SG group [Figure 6].

Western blot assay (quantification of protein expression)

The protein expression and quantification analysis revealed that ZER significantly ($P < 0.05$) downregulated the proinflammatory triggers, including NF-κB together with inducible enzymes COX-2 and iNOS in a dose-dependent manner comparable to that of HCD group [Figure 7]. Besides, the values of protein bands show a reduction in the SG group; however, the data are more significant ($P < 0.05$) in ZIII and ZSG groups.

Seroimmunological analysis of proinflammatory cytokines (ELISA)

The percentage values of TNF-α, IFN-γ, IL-1, and IL-6 were significantly ($P < 0.05$) decreased in all ZER therapeutic groups in a dose-dependent manner compared to the HCD group. On the other hand, SIM treatment also showed significant ($P < 0.05$) anti-inflammatory results in reducing inflammatory mediators. However, the analyzed data demonstrated a more significant ($P < 0.01$) effect on the ZSG group [Table 2].

Table 1: Effect of zerumbone on proinflammatory factors

Experimental groups (n=6)	Mean percentage (pg/ml)			
	TNF-α	IFN-γ	IL-1	IL-6
CN	44.29±1.20	12.19±0.73	13.50±0.87	12.63±0.83
HCD	124.27±1.88	55.39±1.08	46.59±1.36	43.08±1.20
ZPI	88.33±1.19*	47.20±1.25*	37.06±1.62*	33.93±0.82*
ZPII	79.29±1.37*	33.46±0.77*	31.58±1.18*	27.52±1.13*
ZPIII	72.86±1.06#	30.60±1.47#	25.62±1.40#	23.13±0.85#

Each value represents the mean percentage of inflammatory cytokines expression±SEM (%), where n=6. *A statistical significance at P<0.05 and #A statistical significance at P<0.01. CN: Control negative; HCD: High-cholesterol diet; ZER: Zerumbone; ZP: ZER-preventive groups (I, II, and III) (8, 16, and 20 mg/kg/body weight); TNF-α: tumor necrosis factor-alpha; IFN-γ: Interferon gamma; IL: Interleukin; SEM: Standard error of mean

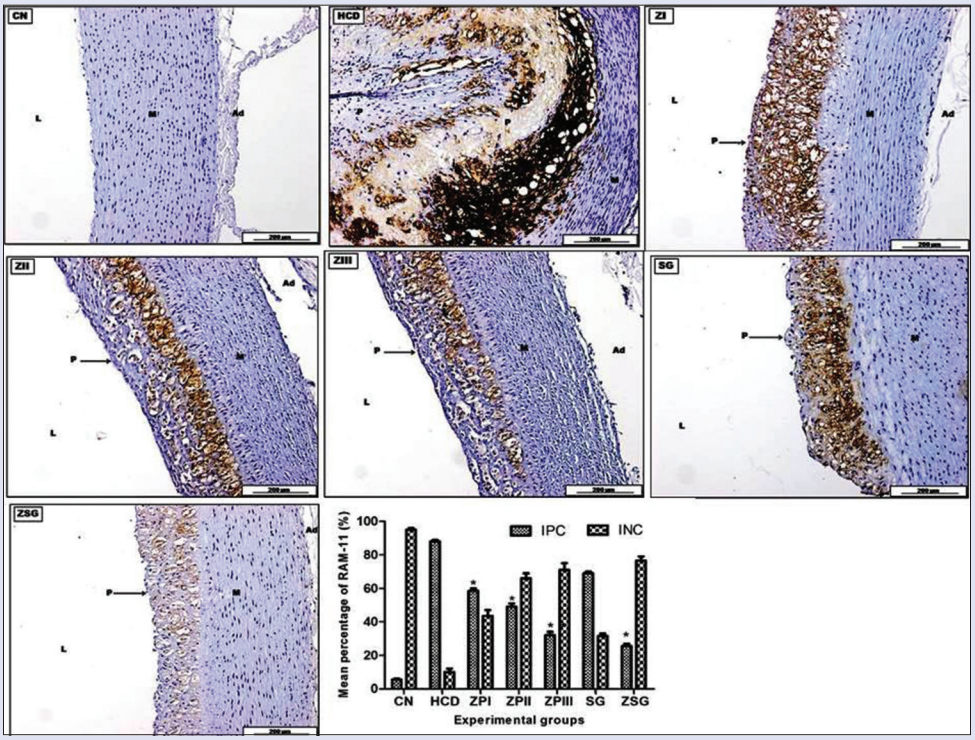

Figure 5: Photomicrograph of thoracic aortas represent immunohistochemical staining with RAM-11 antibody from CN, HCD, ZI, ZII, ZIII, SG and ZSG groups. CN shows no IPC. HCD displays massive and diffuse IPCs within thick rising plaque (p) indicated by deep brownish-stained macrophages (black and yellow arrows). Aortas in ZPI, ZPII, and ZPIII groups demonstrate a significant reduction in plaque size (p) and the intensity of brownish color RAM-11 immunopositive foam cells compare to the thick plaque in HCD (black arrows). There is no reaction in the muscularis layer (m). However, ZSG group compared to SG group had shown a significant reduction in macrophage expression within the intimal plaque. Bar graph represents the quantification assay of IPC and INC. *indicates statistical significance compared to HCD at $P < 0.05$. L: Lumen; M: Media; A: Adventitia. Scale bars: 200 µm. CN: Control group; RAM-11: Regulation of ACE2 and morphogenesis 11; ZP: ZER-preventive; ZER: Zerumbone; IPC: Immunoreactive-positive cells; INC: Immunoreactive-negative cells

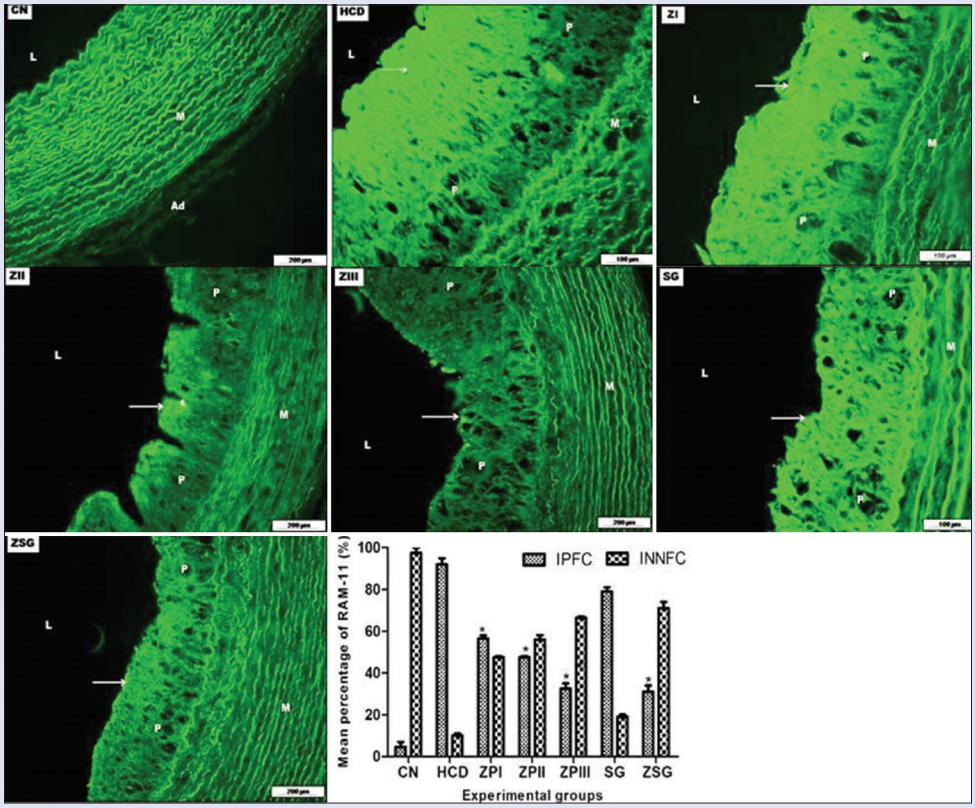

Figure 6: Photomicrograph of thoracic aortas from CN, HCD, ZI, ZII, ZIII, SG and ZSG groups symbolize immunoflourescent staining with RAM-11 antibody. The Control group shows no immunopositive reaction. HCD group demonstrates pronounced immunofluorescent positive reactive cells with increase intensity and percentage of greenish-fluorochrome foam cells in the intimal plaque (p). Aortas in ZPI, II and III groups demonstrate a significant reduction in the macrophage-derived foam cells within the tunica intima compare to HCD group, indicated by low intensity of greenish-fluorochrome immunopositive RAM-11 cells in the intimal plaque (p) (white arrows). However, ZSG group compared to SG group had showed significant lessening in the intensity and percentage of immunofluorescent positive area compare to HCD group. Bar graph represents IPFC and INNFC of macrophage-specific protein biomarker RAM-11. *indicates statistical significance compared to HCD at $P < 0.05$. L: Lumen; M: Media; A: Adventitia. Scale bars: 200 μm. CN: Control group; RAM-11: Regulation of ACE2 and morphogenesis 11; ZP: ZER-preventive; ZER: Zerumbone; IPC: Immunoreactive-positive cells; INC: Immunoreactive-negative cells; IPFC: Immunopositive fluorescent cells; INNFC: Immunonegative nonfluorescent cells

Table 2: Effect of zerumbone and simvastatin treatment on proinflammatory cytokines

Experimental groups (n=6)	Mean percentage (pg/ml)			
	TNF-α	IFN- γ	IL-1	IL-6
CN	40.19±1.46	13.47±0.61	13.06±0.78	12.63±0.83
HCD	113.11±1.81	50.67±1.75	50.94±1.55	47.41±1.42
ZI	96.22±1.06*	41.40±0.93*	39.14±1.03*	41.00±1.034*
ZII	86.36±0.94*	35.27±1.02*	33.96±0.95*	34.54±0.99*
ZIII	77.39±1.28#	31.09±1.08#	30.95±0.68#	33.05±0.65*
SG	75.96±1.58*	39.26±0.82*	40.00±0.92*	39.55±1.53*
ZSG	59.90±1.36#	29.01±1.79#	27.37±1.23#	27.41±0.94#

Each value represents mean percentage of inflammatory cytokines expression±SE (%), where n=6. *A statistical significance at P<0.05 and #A statistical significance at P<0.01. CN: Control negative; HCD: High-cholesterol diet; Z: Zerumbone treated groups (I, II, and III) (8, 16, and 20 mg/kg/body weight), SIM: Simvastatin; SG: SIM group (15 mg/kg); ZER: Zerumbone; ZSG: ZER-SIM group (ZER: 16 mg/kg) and (SIM: 5 mg/kg); SE: Standard error

DISCUSSION

Atherosclerosis is a multifactorial, vascular proliferative disease associated with different risk factors.[16] Hypercholesterolemia is a major risk factor for atherosclerosis, and reduction in plasma cholesterol concentration by drug therapy has reduced atherosclerosis.[17] Many studies prove that chronic inflammation plays a vital role both in the formation and development of atherosclerotic plaque and its thrombotic complications.[18] Hence, understating the importance of inflammation during all stages of atherosclerosis is a crucial demand.[19]

Natural products and their active principles, as sources for new drug discovery in disease prevention and treatment, have attracted considerable attention in recent years due to their effectiveness and safety profile.[20] ZER is an active natural compound that exhibits antiproliferative and anti-inflammatory activities and mediates its activity through the modulation of NF-κB activation.[12] Activated NF-κB is present in atherosclerotic lesion, particularly within smooth muscle cells, macrophages, and endothelial cells, whereas little or no activated NF-κB can be distinguished in arterial wall lacking atherosclerosis.[21] Activated transcriptional factor NF-κB promotes the liberation of more proinflammatory mediators that in turn activate endothelial cells and upregulate overexpression of adhesion molecules.[22]

Thus, in the current study, the primary role of ZER in suppressing NF-κB as an inflammatory modulator in the process of atherogenesis was evaluated. ZER exhibits anti-inflammatory activity through the modulation of NF-κB activity, in which ZER significantly abolishes NF-κB expression in the aortas of supplemented animals as a preventive as well as therapeutic measure. Moreover, a reduction in macrophage and

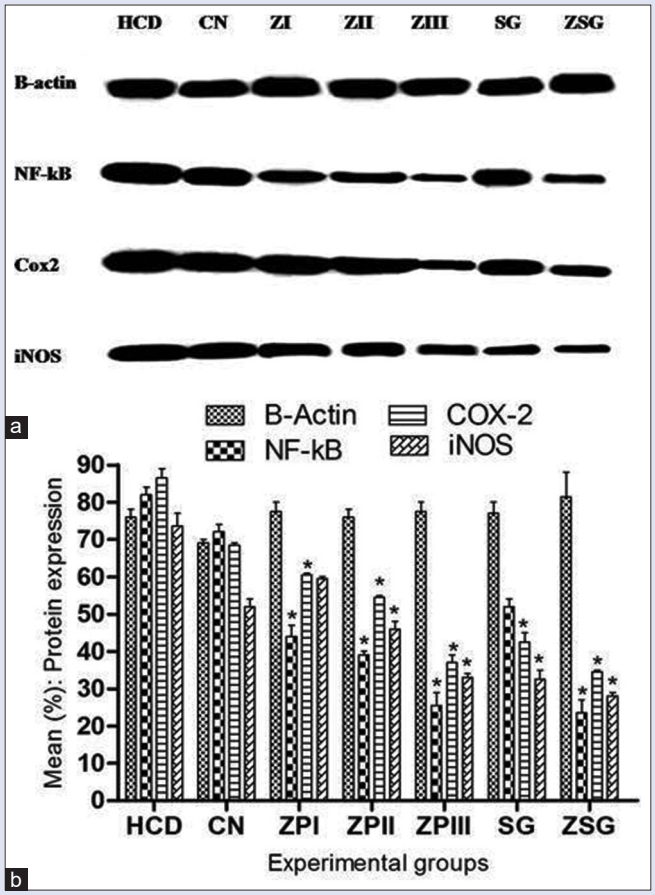

Figure 7: (a) Western blot image analysis from aortic tissue for NF-κB, COX-2, and iNOS. All ZER-supplemented groups and ZSG show a significant reduction in the protein band thickness, indicating downregulation of protein expression. (b) Bar graph represents protein transcription analysis in aortic tissue by Western blotting assay using Image J software. Data reveal significant ($P < 0.05$) suppression of NF-κB, COX-2, and iNOS proteins in treatment groups compare to that of HCD group. ZER: Zerumbone; NF-κB: Nuclear factor kappa-light-chain-enhancer of activated B-cells; COX-2: Cyclooxygenase-2; iNOS: Inducible nitric oxide synthase

VSMCs population within the plaque by ZER resulted in suppression of NF-κB expression.[23]

ZER also inhibits the expression of NF-κB-regulated genes in correlation with the suppression of antiapoptotic gene and TNF-induced invasion activity and upregulates proapoptotic gene expression. Furthermore, the reduction in atherosclerosis lesion and plaque built up is due to the potent anti-inflammatory effect of ZER.[23]

COX-2 is expressed in response to inflammatory cytokines and is increased in atherosclerotic lesion that is characterized by high inflammatory content.[24] The expression of COX-2 is controlled by the NF-κB.[25] Hypercholesterolemia and elevated plasma ox-LDL can stimulate the inflammatory response of vascular wall cells via activation of the NF-κB.[26] Therefore, in the present study, ZER downregulates the expression of COX-2 within the aortic tissue exposed to the high-cholesterol diet via suppression of NF-κB. Thus, our findings are comparable to other investigations regarding NF-κB as well as COX-2 suppression by ZER.[27]

Initiation and propagation of atherosclerosis involve the expression of iNOS in early and advanced atherosclerotic plaques.[28] iNOS produces high amounts of nitric oxide (NO), highly reactive with other free radicals such as superoxide union.[29] Therefore, the predominant role of iNOS in the process of atherogenesis is thought to be related to oxidative stress damage to the vascular endothelial cells.[30] Our data show that ZER significantly averts and reduces iNOS expression in the prophylactic and treatment experimental trials. Moreover, iNOS downregulation by ZER is probably due to NF-κB suppression, which prevents NO production.[9] Besides, our results here are equivalent to other studies suggesting that ZER inhibits NF-κB and iNOS expression is concomitant with the inhibition of NO free radicals generation within activated inflammatory leukocytes.[24,31]

ZER could be a potential component against inflammatory ailments.[32] Based on the fact that atherosclerosis is inflammatory disorder,[33] ZER has been considered in the current investigation. Several cytokines and proinflammatory mediators released by activated plaques such as lipid-laden macrophages, adhered monocytes, T-cells, endothelial cells, and transmigrated SMCs that activate NF-κB.[34] Furthermore, activated T-cells produce IFN-γ that can halt collagen synthesis by the SMCs, limiting its capacity to renovate the collagenous cap, and reinforce the plaque strength which renders the plaque more vulnerable to rupture.[35]

In the current study, proinflammatory cytokines (TNF-α, IFN-γ, IL-6, and IL-1) expressed by inflammatory leukocytes within the plaque lesion such as macrophages and lymphocytes. ZER supplementation alone or in combination with SIM proves a considerable reduction in these cytokines, thus proving the anti-inflammatory potential of ZER in reducing inflammatory reaction.[36-38] Hence, we conclude that the anti-inflammatory effect of ZER may be due to the inhibition of NF-κB expression by this active compound.[9]

Furthermore, the anti-inflammatory potential of ZER was evaluated to estimate a macrophage assemblage biomarker (RAM-11). As a result, ZER significantly reduces the RAM-11 expression within the plaque. The antimacrophage impact of ZER is probably due to its potent anti-inflammatory effect in downregulating transcription factor NF-κB protein expression, particularly in combination with simvastatin as an anti-inflammatory potential, thus suppressing the proinflammatory cytokines releasing, through a reduction in macrophage population within the plaque.[39-41]

CONCLUSION

In the present study, it was recognized that oral administration of ZER, as a single prophylactic regimen and as a supplementary therapeutic measure with SIM antagonistic toward atheromas plaque formation and dissemination, proved to possess a significant antiatherogenic efficacy in averting and reducing the severity of the lesion in a time and dose-dependent manner. At the same time, ZER significantly reduces macrophages assembling within the lesions through a significant reduction in the proinflammatory mediators and cytokines, consequently preventing foam cell formation and plaque progression.

Acknowledgements

The authors would like to express their most generous gratitude and appreciation to the Postmortem and Histopathology Laboratories and Animal House Unit, Faculty of Veterinary Medicine, UPM, for providing places, instruments, chemicals, and consumables for conducting the current experiments.

Financial support and sponsorship

This research work has been financially supported by a grant from the UPM (Grant No. RUGS-5450334).

Conflicts of interest

There are no conflicts of interest.

REFERENCES

1. Jang YJ, Park B, Lee HW, Park HJ, Koo HJ, Kim BO, *et al.* Sinigrin attenuates the progression of atherosclerosis in ApoE−/− mice fed a high-cholesterol diet potentially by inhibiting VCAM-1 expression. Chem Biol Interact 2017;272:28-36.
2. Buckley ML, Williams JO, Chan YH, Laubertová L, Gallagher H, Moss JW, *et al.* The interleukin-33-mediated inhibition of expression of two key genes implicated in atherosclerosis in human macrophages requires MAP kinase, phosphoinositide 3-kinase and nuclear factor-κB signaling pathways. Sci Rep 2019;9:1-12.
3. Falk E. Pathogenesis of atherosclerosis. J Am Coll Cardiol 2006;47:C7-12.
4. Devaraj S, Singh U, Jialal I. The evolving role of C-reactive protein in atherothrombosis. Clin Chem 2009;55:229-38.
5. Chae CW, Kwon YW. Cell signaling and biological pathway in cardiovascular diseases. Arch Pharm Res 2019;42:195-205.
6. Shah PK. Inflammation, infection and atherosclerosis. Trends Cardiovasc Med 2019;29:468-72.
7. Rosa A, Caprioglio D, Isola R, Nieddu M, Appendino G, Falchi AM. Dietary zerumbone from shampoo ginger: New insights into its antioxidant and anticancer activity. Food Funct 2019;10:1629-42.
8. Haque MA, Jantan I, Arshad L, Bukhari SN. Exploring the immunomodulatory and anticancer properties of zerumbone. Food Funct 2017;8:3410-31.
9. Hwang S, Jo M, Hong JE, Park CO, Lee CG, Yun M, *et al.* Zerumbone suppresses enterotoxigenic bacteroides fragilis infection-induced colonic inflammation through inhibition of NF-κB. Int J Mol Sci 2019;20:4560.
10. Utaka Y, Kashiwazaki G, Tajima S, Fujiwara Y, Sumi K, Itoh T, *et al.* Antiproliferative effects of zerumbone-pendant derivatives on human T-cell lymphoid cell line Jurkat cells. Tetrahedron 2019;75:1343-50.
11. Girisa S, Shabnam B, Monisha J, Fan L, Halim CE, Arfuso F, *et al.* Potential of zerumbone as an anti-cancer agent. Molecules 2019;24:E734.
12. Singh SP, Nongalleima K, Singh NI, Doley P, Singh CB, Singh TR, *et al.* Zerumbone reduces proliferation of HCT116 colon cancer cells by inhibition of TNF-alpha. Sci Rep 2018;8:4090.
13. Kim MJ, Yun JM. Molecular mechanism of the protective effect of zerumbone on lipopolysaccharide-induced inflammation of THP-1 cell-derived macrophages. J Med Food 2019;22:62-73.
14. Hemn HO, Noordin MM, Rahman HS, Hazilawati H, Zuki A, Chartrand MS. Antihypercholesterolemic and antioxidant efficacies of zerumbone on the formation, development, and establishment of atherosclerosis in cholesterol-fed rabbits. Drug Des Devel Ther 2015;9:4173-208.
15. Fruebis J, Silvestre M, Shelton D, Napoli C, Palinski W. Inhibition of VCAM-1 expression in the arterial wall is shared by structurally different antioxidants that reduce early atherosclerosis in NZW rabbits. J Lipid Res 1999;40:1958-66.
16. Ketelhuth DF. The immunometabolic role of indoleamine 2,3-dioxygenase in atherosclerotic cardiovascular disease: Immune homeostatic mechanisms in the artery wall. Cardiovasc Res 2019;115:1408-15.
17. Dorighello GG, Inada NM, Paim BA, Pardo-Andreu GL, Vercesi AE, Oliveira HC. *Mangifera indica* L. extract (Vimang®) reduces plasma and liver cholesterol and leucocyte oxidative stress in hypercholesterolemic LDL receptor deficient mice. Cell Biol Int 2018;42:747-53.
18. Baumer Y, McCurdy S, Weatherby TM, Mehta NN, Halbherr S, Halbherr P, *et al.* Hyperlipidemia-induced cholesterol crystal production by endothelial cells promotes atherogenesis. Nat Commun 2017;8:1129.
19. Obermayer G, Afonyushkin T, Binder CJ. Oxidized low-density lipoprotein in inflammation-driven thrombosis. J Thromb Haemost 2018;16:418-28.
20. Khan MS, Ahmad I. Herbal medicine: current trends and future prospects. In New Look to Phytomedicine. Academic Press; Elsevier; 2019. p. 3-13.
21. Serasanambati M, Chilakapati SR. Function of nuclear factor kappa B (NF-kB) in human diseases – A review. South Indian J Biol Sci 2016;2:368-87.
22. Chistiakov DA, Orekhov AN, Bobryshev YV. Vascular smooth muscle cell in atherosclerosis. Acta Physiol (Oxf) 2015;214:33-50.
23. Varghese JF, Patel R, Singh M, Yadav UC. "Herbal Intervention in Cardiovascular Diseases." In Functional Food and Human Health. Springer, Singapore: 2018. p. 277-96.
24. Chen L, Deng H, Cui H, Fang J, Zuo Z, Deng J, *et al.* Inflammatory responses and inflammation-associated diseases in organs. Oncotarget 2018;9:7204-18.
25. Grancieri M, Martino HS, Gonzalez de Mejia E. Chia (*Salvia hispanica* L.) seed total protein and protein fractions digests reduce biomarkers of inflammation and atherosclerosis in macrophages *in vitro*. Mol Nutr Food Res 2019;63:e1900021.
26. Schwarz A, Bonaterra GA, Schwarzbach H, Kinscherf R. Oxidized LDL-induced JAB1 influences NF-κB independent inflammatory signaling in human macrophages during foam cell formation. J Biomed Sci 2017;24:12.
27. Haque MA, Jantan I, Harikrishnan H, Ghazalee S. Standardized extract of *Zingiber zerumbet* suppresses LPS-induced pro-inflammatory responses through NF-κB, MAPK and PI3K-Akt signaling pathways in U937 macrophages. Phytomed 2019;54:195-205.
28. Pathak P, Kanshana JS, Kanuri B, Rebello SC, Aggarwal H, Jagavelu K, *et al.* Vasoreactivity of isolated aortic rings from dyslipidemic and insulin resistant inducible nitric oxide synthase knockout mice. Eur J Pharmacol 2019;855:90-7.
29. Gliozzi M, Scicchitano M, Bosco F, Musolino V, Carresi C, Scarano F, *et al.* Modulation of nitric oxide synthases by oxidized LDLs: Role in vascular inflammation and atherosclerosis development. Int J Mol Sci 2019;20:E3294.
30. Yang S, Liu L, Meng L, Hu X. Capsaicin is beneficial to hyperlipidemia, oxidative stress, endothelial dysfunction, and atherosclerosis in Guinea pigs fed on a high-fat diet. Chem Biol Interact 2019;297:1-7.
31. Murakami A, Ohigashi H. Targeting NOX, INOS and COX-2 in inflammatory cells: Chemoprevention using food phytochemicals. Int J Cancer 2007;121:2357-63.
32. Wang M, Niu J, Ou L, Deng B, Wang Y, Li S. Zerumbone protects against carbon tetrachloride (CCl4)-induced acute liver injury in mice via inhibiting oxidative stress and the inflammatory response: Involving the TLR4/NF-κB/COX-2 pathway. Molecules 2019;24:1964.
33. Bäck M, Yurdagul A Jr., Tabas I, Öörni K, Kovanen PT. Inflammation and its resolution in atherosclerosis: Mediators and therapeutic opportunities. Nat Rev Cardiol 2019;16:389-406.
34. Gholipour S, Sewell RD, Lorigooini Z, Rafieian-Kopaei M. Medicinal plants and atherosclerosis: A review molecular aspects. Curr Pharm Des 2018;24:3123-31.
35. Bartlett B, Ludewick HP, Misra A, Lee S, Dwivedi G. Macrophages and T cells in atherosclerosis: A translational perspective. Am J Physiol Heart Circ Physiol 2019;317:H375-86.
36. Al-Saffar F, Ganabadi S, Fakurazi S, Yaakub H, Lip M. Chondroprotective effect of zerumbone on monosodium iodoacetate induced osteoarthritis in rats. J Appl Sci 2010;10:248-60.
37. Zakaria ZA, Mohamad AS, Ahmad MS, Mokhtar AF, Israf DA, Lajis NH, *et al.* Preliminary analysis of the anti-inflammatory activity of essential oils of *Zingiber zerumbet*. Biol Res Nurs 2011;13:425-32.
38. Tzeng TF, Liou SS, Chang CJ, Liu IM. Zerumbone, a tropical ginger sesquiterpene, ameliorates streptozotocin-induced diabetic nephropathy in rats by reducing the hyperglycemia-induced inflammatory response. Nutr Metab (Lond) 2013;10:64.
39. Sulaiman MR, Perimal EK, Akhtar MN, Mohamad AS, Khalid MH, Tasrip NA, *et al.* Anti-inflammatory effect of zerumbone on acute and chronic inflammation models in mice. Fitoterapia 2010;81:855-8.
40. Chen BY, Lin DP, Wu CY, Teng MC, Sun CY, Tsai YT, *et al.* Dietary zerumbone prevents mouse cornea from UVB-induced photokeratitis through inhibition of NF-κB, iNOS, and TNF-α expression and reduction of MDA accumulation. Mol Vis 2011;17:854-63.
41. Abdelwahab SI, Abdul AB, Zain ZN, Hadi AH. Zerumbone inhibits interleukin-6 and induces apoptosis and cell cycle arrest in ovarian and cervical cancer cells. Int Immunopharmacol 2012;12:594-602.